Cement and Concrete Composites 143 (2023) 105249

Contents lists available at ScienceDirect

Cement and Concrete Composites

journal homepage: www.elsevier.com/locate/cemconcomp

Crack monitoring strategy for concrete structures in various service conditions via multiple CNT-CF/cement composite sensors: Experiment and simulation approaches

Million Tafesse [a], Abel Shiferaw Alemu [b], Beomjoo Yang [c], Solmoi Park [d], Hyeong-Ki Kim [b,*]

[a] Research and Development Division, MC-Bauchemie Manufacturing Plc, Addis Ababa, 5452, Ethiopia
[b] Department of Architectural Engineering, Chosun University, 309 Pilmun-daero, Dong-gu, Gwangju, 61452, Republic of Korea
[c] School of Civil Engineering, Chungbuk National University, Chungdae-ro 1, Seowon-gu, Cheongju, Chungbuk, 28644, Republic of Korea
[d] Department of Civil Engineering, Pukyong National University, 45 Yongso-ro, Nam-gu, Busan, 48513, Republic of Korea

ARTICLE INFO

Keywords:
Monitoring
Crack
Carbon nanotube
Conductive cement composites
FEM simulation

ABSTRACT

A crack monitoring strategy using parallelly-arranged multiple conductive cement composites for reinforced concrete was verified through a series of experiments and simulations. First, the electrical resistances of various locations of the mortar embedding the CNT-CF/composites were measured along with changes in humidity. Then, shear and flexural cracks were generated through a bending test of the reinforced mortar in which the CNT-CF/cement composite bars were embedded. The change in resistance of the composite bars themselves and between adjacent composite bars before and after cracking was measured. Differences in the results with the cracks in dried, wet, and also self-healing conditions were compared. Additionally, a finite element simulation on the electrical resistance under the experimental conditions was conducted to better understand the measurement results. Based on these experimental and simulation results, the strategy for monitoring structural damage under various operating scenarios was discussed. It was possible to monitor cracks of the reinforced mortar by detecting the increases and/or fluctuations in resistances of the composite bars themselves and between adjacent composite bars.

1. Introduction

Over the past decade, numerous studies have been conducted to develop cement composites with excellent electrical conductivity that can function as multi-purpose sensors for concrete structures [1]. Due to the size effect, nano-sized inclusions such as carbon nanotubes (CNTs) or graphene formed better electrical-conductive networks in the cement matrix with lower contents compared to larger carbon materials, such as carbon fiber or graphite particles [2]. As a result, the percolation threshold of carbon nanomaterials is much lower than that of larger materials, making them less likely to impact the mechanical properties of the cement matrix and the durability of the structure [3]. Furthermore, the conductive networks of carbon nanomaterials are effectively arranged between the hydration products, so electrical conductivity is not likely to be degraded by further hydration as the networks are not blocked by nucleation and growth of the hydration products [4]. This makes the cement composites with carbon nanomaterials reliable in terms of mechanical and electrical properties.

These cement composites with excellent electrical conductivity can be installed on the surface of or inside reinforced concrete structures in the form of sensors for various purposes, such as measuring pressure, monitoring penetration of chloride or carbonation, and sensing cracking [5,6]. The cement composite sensors exhibit physical and chemical behavior similar to that of concrete, allowing monitoring of the structure's behavior by measuring the change in electrical signal of the sensor [4]. The cracking of concrete also leads to the cracking of the cement composite sensors embedded in the concrete structure, leading to a decrease in conductivity. As a result, structural degradation and durability of the reinforced concrete structures can be monitored by measuring the change in electrical behavior [1].

Previous studies have shown that the electrical resistance of conductive cement composites containing carbon nanomaterials increases rapidly with the initiation of cracks in concrete. In our study [7], a highly conductive CNT/cement composite was fabricated using a

* Corresponding author.
E-mail address: hyeongki@chosun.ac.kr (H.-K. Kim).

https://doi.org/10.1016/j.cemconcomp.2023.105249
Received 6 April 2023; Received in revised form 25 July 2023; Accepted 12 August 2023
Available online 15 August 2023

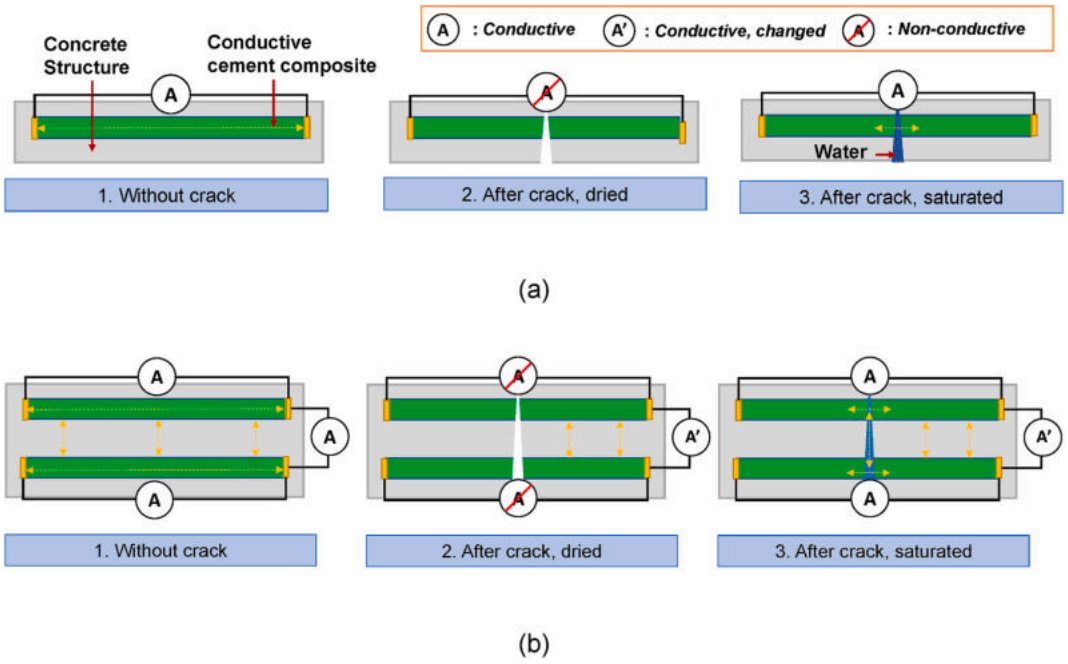

Fig. 1. Concept on the crack monitoring using conductive cement composite sensors based on service scenarios of concrete structures (a) with single composite in Ref. [7]): and (b) with parallelly-arranged multiple composite in the present work, the yellow arrows indicate the conductive pathway. (For interpretation of the references to color in this figure legend, the reader is referred to the Web version of this article.)

Table 1
Mix proportions used and their properties (also shown in Ref. [13]).

Category	Weight ratio							Resistivity (Ω·cm)	
	C	W	S	SF	SP	CNT	CF	Saturated	Vacuum dried[a]
Composite sensor	1	0.4	1	0.1	0.9%	0.6%	2%	5-13 × 10^0	
Embedding mortar	1	0.45	2	-	0.4	-	-	10^3–10^4	10^6–10^7

[a] Vacuum-dried at 50 °C for 3 days.

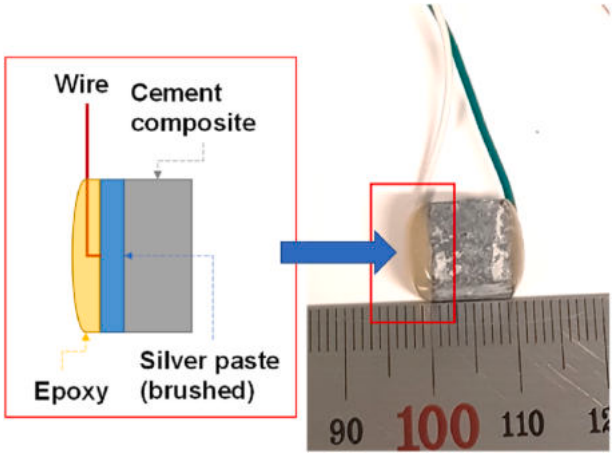

Fig. 2. Details in connection of wire with CNT-CF/cement composites (redrawn from Ref. [13]).

'one-step mixing method', without applying complex dispersion methods such as sonication or use of surfactants. Its electrical resistance ranged from 10^0 to 10^2 Ωm (=0-2 log[Ωm]), which is comparable to that of semiconductors, whereas that of concrete is about 10^4-10^8 Ωm (=4-8 log[Ωm]) [7]. Due to cracking, the resistivity of the composite drastically increased up to 10^6-10^8 Ωm (=6-8 log[Ωm]), which was almost overload [7]. Similar experimental results have been reported in the literature, with conductive cement composites being tested for their ability to monitor cracks in concrete. Ding [8] investigated the relationship between electrical resistance and cracks of cement composites containing nano carbon black, steel fiber, and carbon fiber to apply self-sensing material. Chen [9] used cement composites with carbon fiber and graphite for the same purpose. Downey [10,11] prepared conductive CNT/cement composite plates and implemented multiple electrodes with a certain width and spacing. The plate was damaged by impact, and the crack was traced by measuring the resistance between the multiple electrodes. In most studies, cracks in the conductive cement composite were generated simply through loading, and the increase in electrical resistance was confirmed. Meanwhile, for crack monitoring in the field, the effects of the surrounding environment, such as changes in moisture content, chloride ion penetration, carbonation, and the increase in hydration degree over time, should also be considered. For example, it was found that the electrical resistance of conductive cement composites embedded in reinforced mortar undergoing tensile cracking increased only when the composite was in a dry condition and not when the crack was filled with water, as the moisture in the crack area became a conductive pathway [7,10,12]. As the resistivity of water is generally lower than that of cement composite, the resistance of cracked composite sensor remained constant even after cracking when the crack was saturated. Therefore, there is a limit to monitoring the occurrence of cracks with only single conductive cement composite sensor.

To overcome this limitation, a new monitoring methodology and strategy that applies multiple conductive cement composite sensors were established in this study. The use of multiple composite sensors enables monitoring of the resistance change not only for the sensors

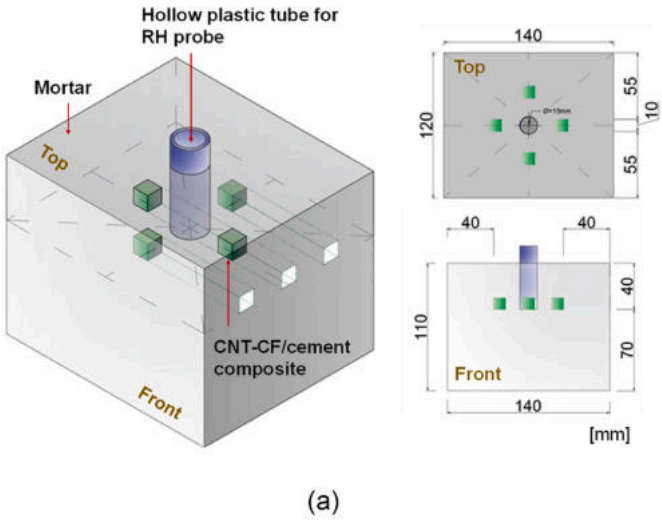

Fig. 3. Mortar specimens embedding the CNT-CF/cement composites to investigate effect of internal relative humidity on the resistance of the composites and mortar (Test M): (a) schematic diagram and (b) actual specimen.

themselves, but also between the adjacent composites embedded in concrete. The concepts of the conventional method with a single composite sensor and the proposed method with multiple sensors are

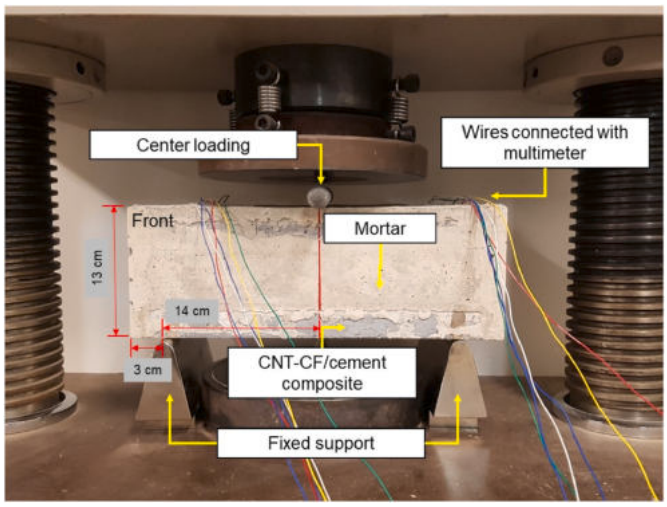

Fig. 5. Three-point bending for the reinforced mortar embedding CNT-CF/cement composites.

illustrated in Fig. 1. When using multiple conductive cement composites, a saturated crack will form a conductive pathway between adjacent composites. The resistance of the composite sensors and those between adjacent sensors may significantly change from their initial values during cracking, even under various conditions in the crack. Therefore, it is expected that the presence of cracks can be more clearly identified through this method. The resistances of the composite sensors and those between adjacent composite sensors may change under various conditions in the crack, and it is expected that cracks can be more clearly identified through this method.

In this study, a crack monitoring strategy using parallelly-arranged multiple conductive cement composites for reinforced concrete was verified through a series of experiments and simulations. First, the electrical resistances of various locations of the mortar embedding the CNT-CF/composites were measured along with changes in humidity. Then, shear and flexural cracks were generated through a bending test of the reinforced mortar in which the CNT-CF/cement composite bars were embedded. The change in resistance of the composite bars themselves and between adjacent composite bars before and after cracking was measured. Differences in the results with the cracks in dried, wet, and also self-healing conditions were compared. Additionally, a finite element simulation on the electrical resistance under the experimental

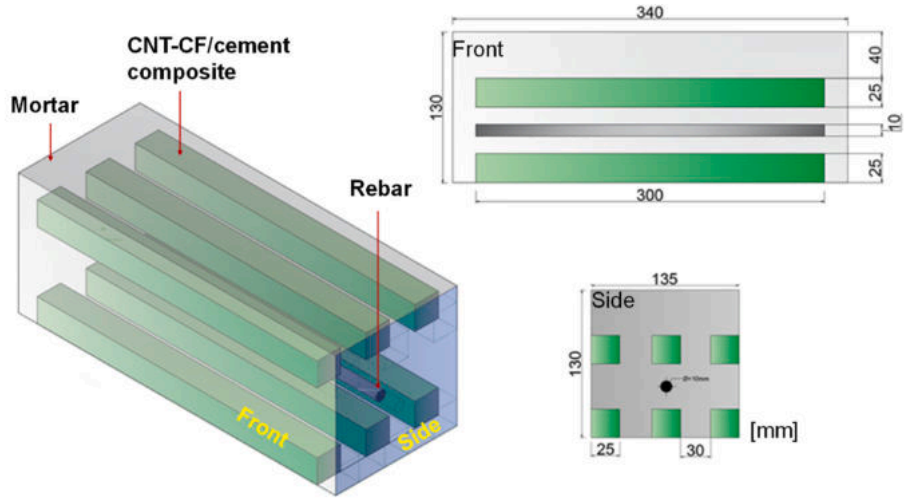

Fig. 4. Schematic diagram of reinforced mortar specimens embedding the CNT-CF/cement composites to investigate effect of cracks on the resistance of the composites and mortar (Test C).

Fig. 6. Crack patterns for the reinforced mortar embedding CNT-CF/cement composites after three-point bending.

conditions was conducted to better understand the measurement results. Based on these experimental and simulation results, the strategy for monitoring structural damage under various operating scenarios was discussed.

2. Materials and method

2.1. Materials and mix proportions

The materials and mix proportion of CNT-CF/cement composite were identical to those in our recent work, which had been optimized in terms of electrical and mechanical properties [13]. For the composite, Type I ordinary Portland cement (C), silica fume (SF), quartz sand (S), multi-walled CNT (CNT), carbon fiber (CF), and superplasticizer (SP) were used. The commercialized cement satisfied Korean Standard (KS) L 5210 and ASTM C 150. The particle size range of sand was within 0.1–0.8 mm, and their specific gravity and water absorption were 2.65 and 0.1%. Commercialized silica fume (Elkem Corp.) with a specific gravity of 2.23 and mean particle size of 220 nm was used. The solid content of the polycarboxylic acid-based superplasticizer was 30%. As a conductive filler, CNT with a diameter of 10–15 nm, length of 10–50 μm, and purity higher than 95% was used (supplied from Kumho Chemical Inc). A 3 mm-length CF (TORAYCA-T700S, Toray) with diameter of 7 μm and purity of 99% was used as a reinforcement to prevent dry shrinkage-induced cracking. For the reinforced mortar, the same cement used for the composite and conventional river sand with specific gravity of 2.60 was used, and then SD400-D10 rebars were prepared.

The mix proportions of composites and mortar are shown in Table 1, along with their average electrical resistivity values obtained from 4 to 6 hardened specimens with dimensions of 15 × 15 × 80 mm^3. The resistivity was measured using an alternative current (AC) impedance meter, and more information on the measurement method and equipment can be found in Ref. [13]. The resistivity of the mixture was constant against temperature change, internal humidity, and further hydration, but changed by long-term chloride penetration or carbonation [1,4].

2.2. Experimental methodology

For the present work, two types of mortar specimens embedding the CNT-CF/cement composite were prepared for different purposes. The first was to evaluate the effect of moisture on the resistance of the composite and mortar before cracking (Test M), and the second was to monitor the cracks (Test C). The composite sensors were produced in two different forms for these two purposes: one in cubic forms with dimensions of 10 × 10 × 10 mm^3 for Test M, and the other in bar forms with dimensions of 25 × 25 × 300 mm^3 (W × H × L) for Test C. For the composite mixtures, all solid materials, including CNT, were dry-mixed for 10 min, and then wet-mixed with water and superplasticizer for an additional 10 min. After pouring the fresh mixture into each mold, it was sealed and cured for 1 day, and then cured in water for 91 days under room temperature to ensure sufficient hydration. As shown in Fig. 2, conductive silver paste was applied to both ends of each of these composite sensors to serve as electrodes. The conductive wires were brushed together, and after the paste hardened, both ends were coated with epoxy to seal the silver paste and wires.

For Test M, a mold with dimensions of 12 × 11 cm × 14 cm^3 (W × H × L) was prepared (Fig. 3), while for Test C, a mold with dimensions of 13 × 13 × 34 cm^3 (W × H × L) was prepared (Fig. 4). Four identical specimens were cast for each test. The mortar for these tests was mixed to have a low flow diameter of 150 mm in accordance with ASTM C 1437. The fresh mortar was well-compacted to the height where the composite sensors were to be placed, and the composite samples were placed on top of it after fixing their position with a nylon string anchored to the mold. The fresh mortar was then covered again, and rod compaction and external vibration with very weak force were applied.

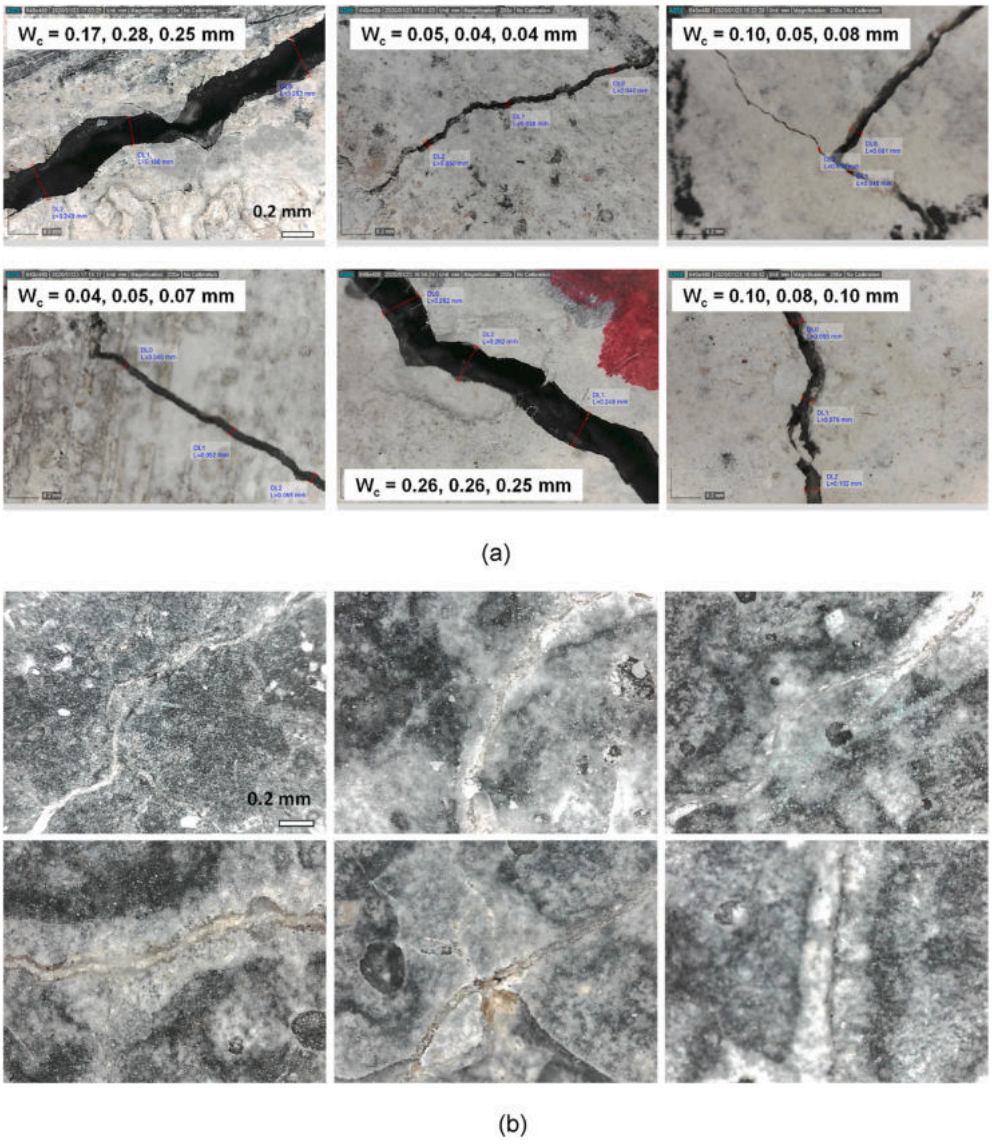

Fig. 7. Magnified images of cracks in the CNT-CF/cement composites embedded in the mortar: (a) immediately after cracking and (b) after self-healing through immersion in water for 91 d.

Table 2
Sequence of the resistance measurement for various points of the reinforced mortar with CNT-CF/cement composites under 3-point bending (Test setup C).

Sequence	Situation	Moisture condition in cracks	Experimental procedure
0	Sample preparation		Sound mortar specimens embedding the composites were water-cured for 91 d
1	Before cracking	Wet	The resistance was measured from specimens directly taken out from the curing water
2		Dried	Specimens were air-dried for 7 d after Sequence 1 and the resistance was measured
3	After cracking	Dried	Mortar specimens after Sequence 2 were re-saturated by immersing in water for 24 h, then three-point bending were applied, and the resistance was measured directly after cracking
4		Wet	Specimens were immersed in water for 1 min again to fill the cracks with water after Sequence 3, and the resistance was measured
5	After self-healing	Wet	Specimens after Sequence 4 were immersed in water to allow them to self-heal, and the resistance was measured after taken out from the water
6		Dried	Specimens after Sequence 5 were air-dried for 7 d before measuring the resistance

Note that the position of the composite samples in the mortar, fabricated with the same method, was confirmed by a destructive method (crushing the mortar specimens) in Ref. [1], and the composite samples were located in the initially embedded position. For the specimens of Test M, a plastic tube with a length of 40 mm and an outer diameter of 15 mm was embedded in the upper side of fresh mortar for measuring the relative humidity in the mortar, and both ends were blocked with a plastic film to prevent the intrusion of mortar (Fig. 3b). For the specimens of Test C, a rebar (SD400, D10) was embedded along with the composite samples. During the fabrication of the sample, this rebar was fixed by a nylon string from the top of the mold to fix the position. The specimens were cured in water at room temperature for 91 days after sealing and curing for a single day.

For Test M, the specimens were placed in a humidity-temperature

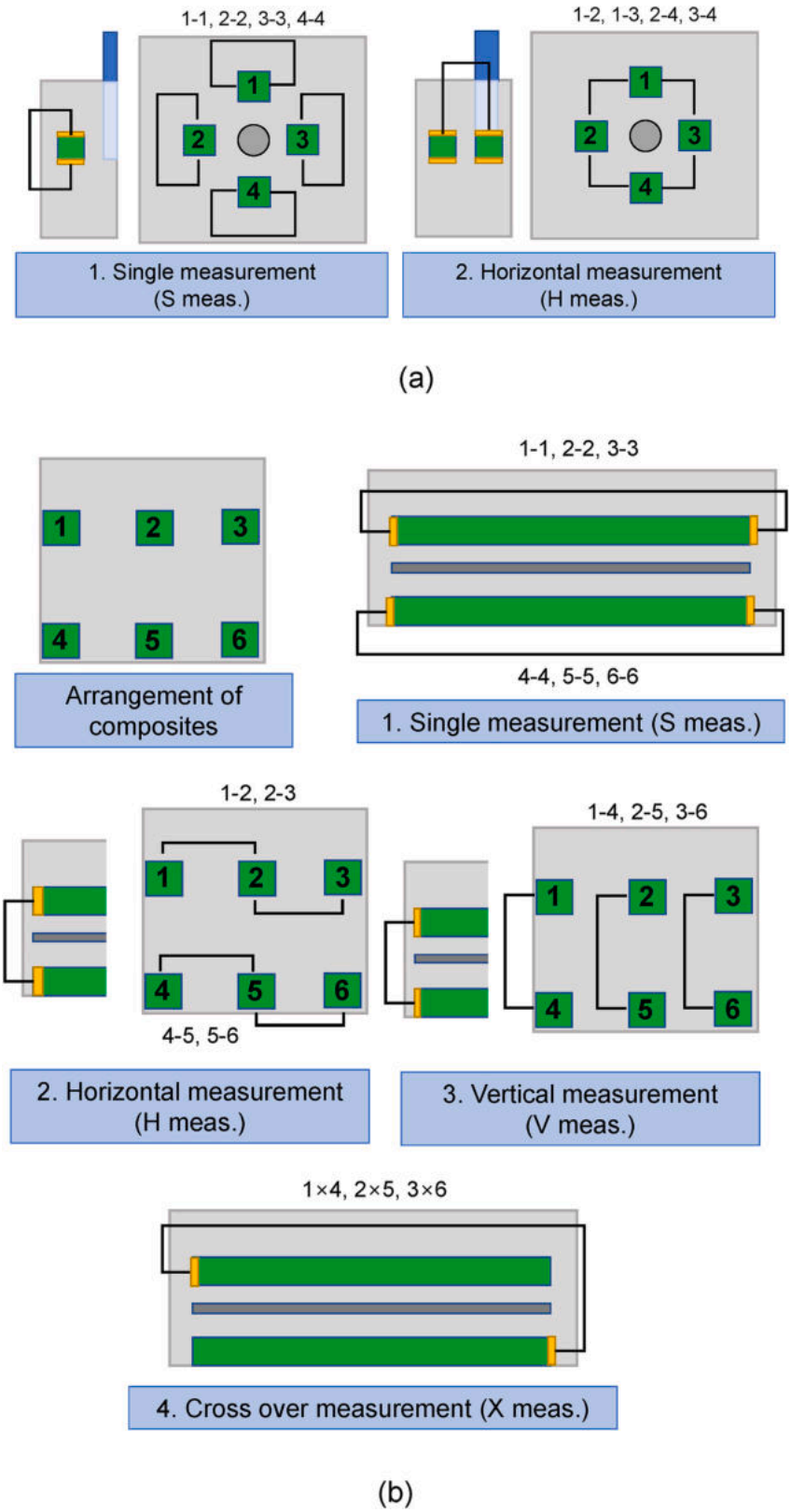

Fig. 8. Measurement directions of the cement composites embedded in the reinforced mortar: Test Setups 1 (a) and 2 (b) (light gray: mortar; dark gray: rebar; green: CNT-CF/cement composites; yellow: electrode; black lines: conductive connection). (For interpretation of the references to color in this figure legend, the reader is referred to the Web version of this article.)

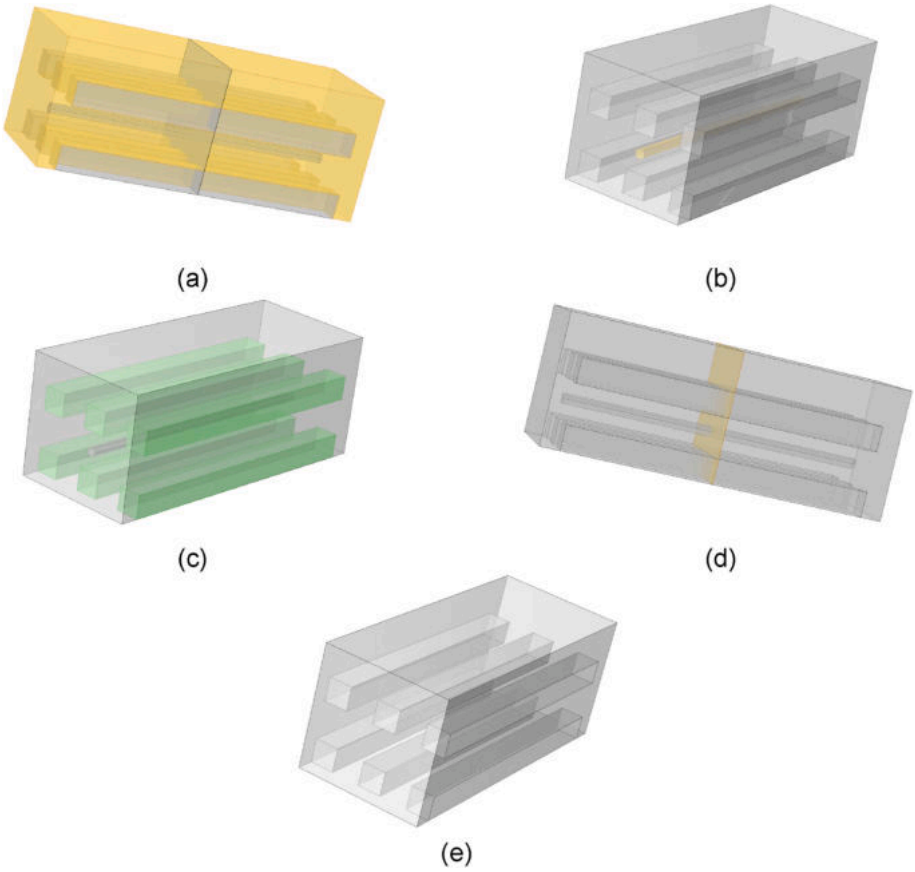

Fig. 9. Configuration of specimen for simulation: (a) surround mortar, (b) rebar, (c) CNT-CF cement composite bars, (d) crack; and (e) specimen without rebar for as reference.

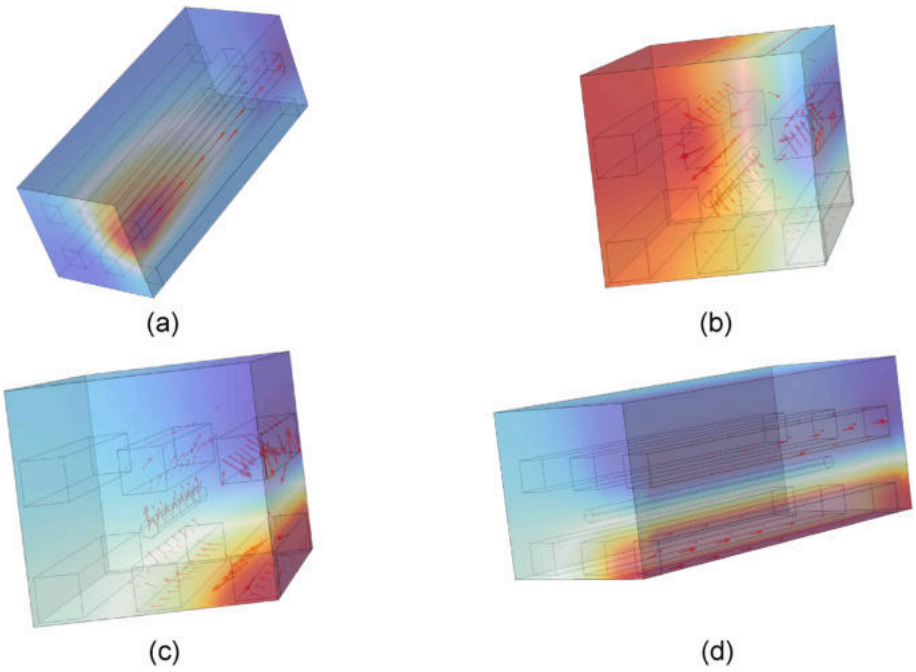

Fig. 10. Simulated current density (contour) and current flow (arrow) for specimens without crack: (a) S, (b) H, (c) V, and (d) X meas.

control chamber with a temperature of 23 °C. The relative humidity in the chamber was gradually lowered from 99%, to 80% and then 50% over a month. This allowed the specimens to dry from all six surfaces. The plastic film covering the plastic tube was removed, and the relative humidity inside the mortar was measured by a probe-type humidity sensor (a Vaisala HNP40S probe connected with a Vaisala HN40

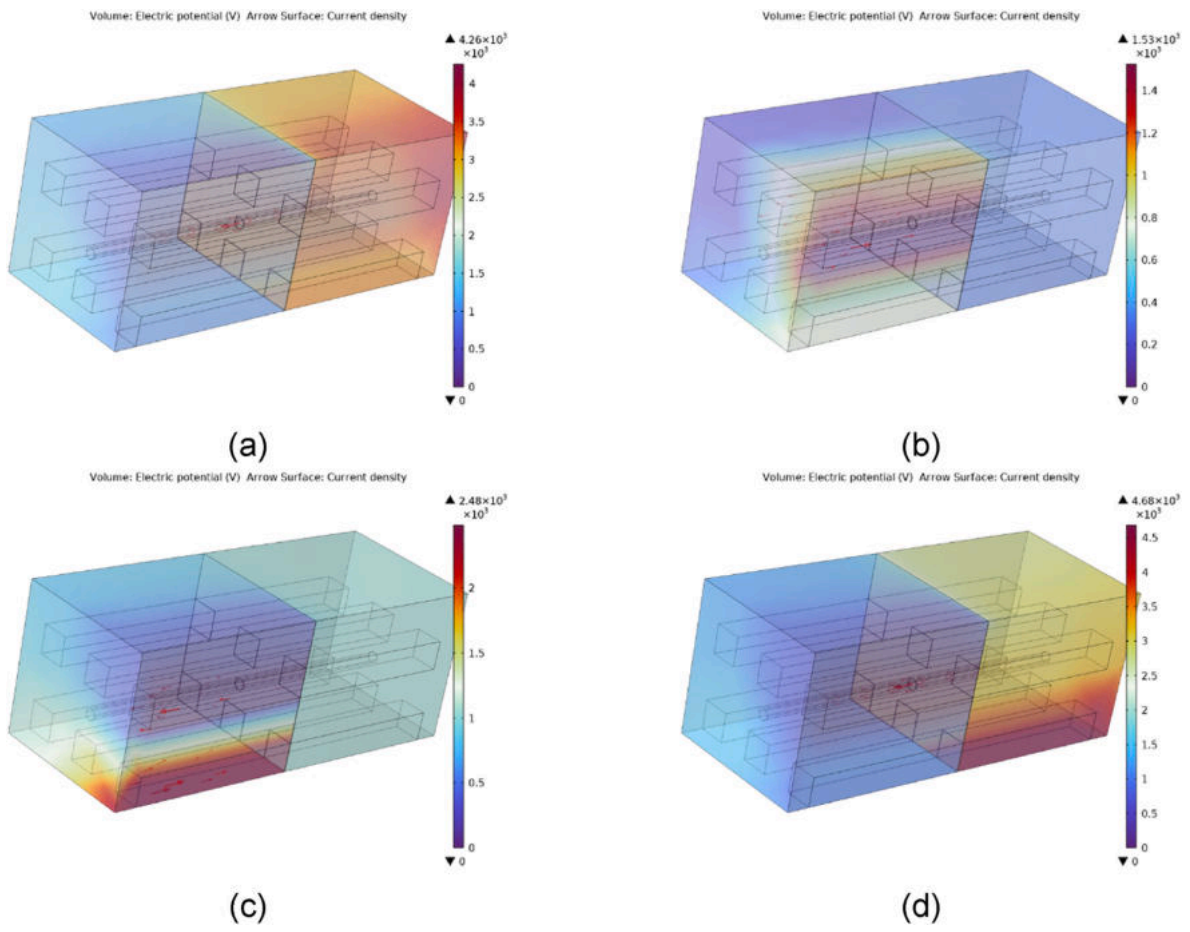

Fig. 11. Simulated current density (contour) and current flow (arrow) for specimens with dried crack: (a) S, (b) H, (c) V, and (d) X meas.

indicator) (Fig. 3b). Humidity and temperature data were collected once a day. After one month, the specimen was placed in a box containing silica gel for another month to further dry the specimens. During the test, not only was the relative humidity inside the mortar measured, but also the relative humidity outside the specimen and within the silica gel after the specimen was immersed in the gel.

For Test C, a 3-point flexural load was applied to the specimens in Fig. 5. Considering the distance from both supports and height in Fig. 5, the specimens were structurally subjected to both bending and shear. The crack patterns of the specimens are shown in Fig. 6. As shown in Fig. 7a, the cracks in the specimens were photographed using a portable USB microscope, and the width was measured. The cracked specimens were then immersed in water for an additional month to induce the cracks to be filled, i.e., to self-heal. The filling of the cracks is shown in Fig. 7b. The detailed sequence for Test C was complicated, so it is summarized in Table 2. In this study, the situation of crack reopening after self-healing was not considered.

During Test M and Test C, the electrical resistance of various locations was measured under different conditions. The types of resistance measured are separately presented in Fig. 8. A single measurement for gauging the resistance of the composite sensor itself, embedded in the mortar, was referred to as "S meas," while horizontal, vertical, and crossover measurements between adjacent composite sensors were designated as "H meas," "V meas," and "X meas," respectively. The electrical resistance was measured using an inductance, capacitance, and resistance (LCR) meter (Keysight E4980AL) over the frequency range of 20 Hz–100 kHz. Note that the imaginary parts of the impedance were much lower than the real parts in the CNT-CF/cement composite, and the real part was considered as the resistance.

3. Numerical simulation

Finite element simulations were conducted to obtain theoretical electrical resistance values under the same conditions as Test C, using commercial software COMSOL Multiphysics® with the AC/DC module (electrical fields and currents). The specimen model used in the simulation had the same dimensions as the specimens in Test C (Fig. 9), and the location of the cement composites was configured as shown in Fig. 4. In addition, a model without reinforcing bars was also simulated to evaluate the effect of rebars on the resistance results. While the experiment had multiple cracks in vertical and diagonal directions, the crack was simply modeled as an isosceles triangular prism layer in the center of the specimen. Electrical property values for each component, including the composite, mortar, rebar, and crack, were assigned using values summarized in Table 4. Most of these values were measured in this study or in our previous works, and some were adopted from general values. Notably, since it was not possible to clearly determine the resistance value for the self-healed crack, it was assumed. The FEM model included the Maxwell equations, including Maxwell-Ampere's law, Faraday's law, Gauss' law, and the equation of continuity. Mesh settings for these CAEs are shown in the Appendix.

Under these conditions, the resistance between the end surfaces of the composite samples, where the electrodes and wires were set in the experiment, was calculated. Figs. 10-12 show the visualized current flow direction and current density of specimens from the numerical calculation. When there was a crack in the dried state, the contour color of the electric density between the split parts facing each other was very different, i.e., the connectivity of the electric density was very low even though there was rebar between the two parts. Meanwhile, when water filled the crack, the color of the contour was uniform even in the cracked

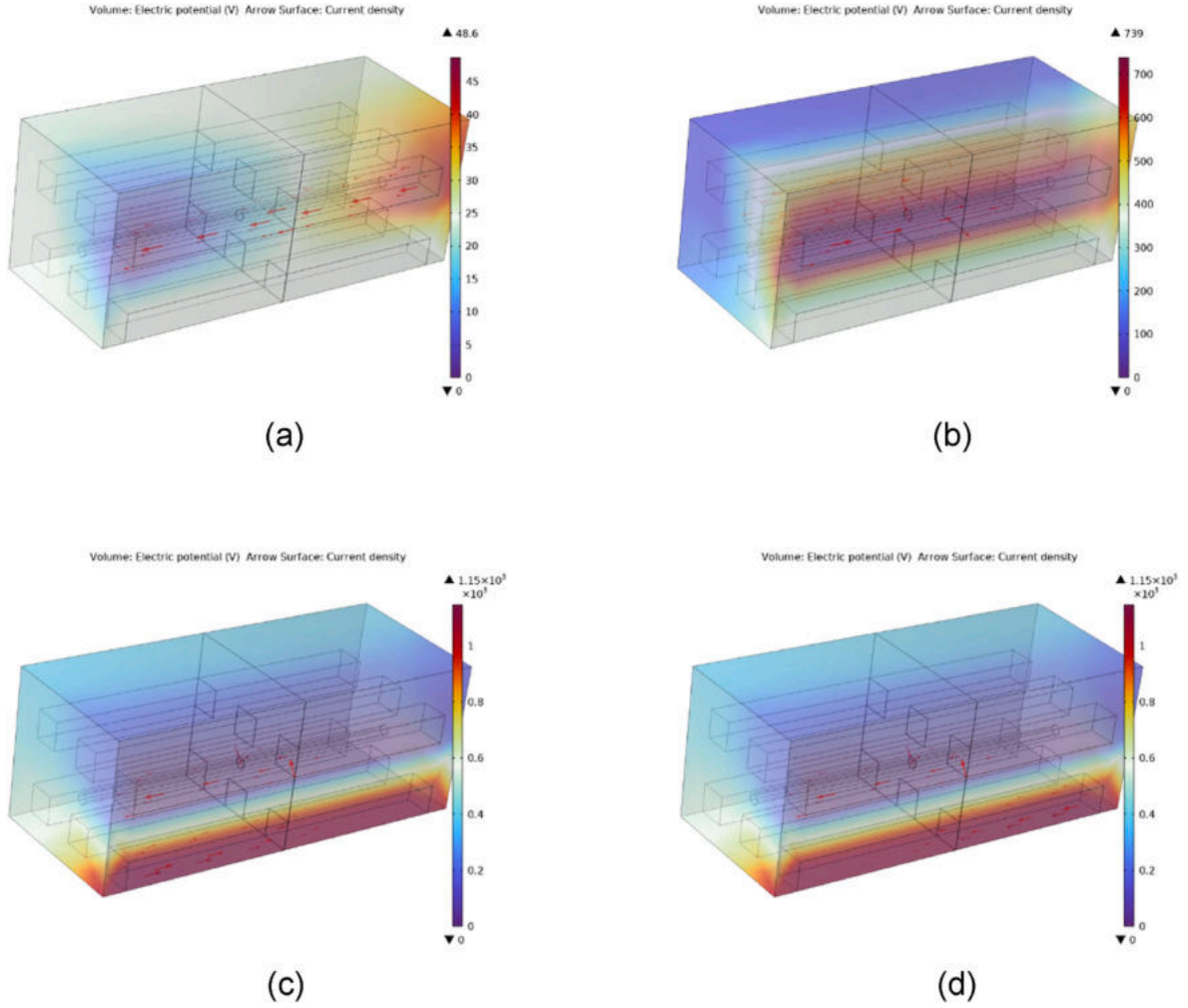

Fig. 12. Simulated current density (contour) and current flow (arrow) for specimens with crack saturated by tap water: (a) S-, (b) H-, (c) V-, and (d) X meas.

part, indicating that the electrical density connectivity was high. This suggests that the moisture condition in the crack greatly affects the connectivity.

A comparison between the resistance measured by the experiment and that from the simulation is discussed in a later section. An important point to consider when comparing the experimental results with the simulation results is that the simulation conditions did not perfectly reflect the actual experimental conditions. For example, in the actual specimens, the cracks with narrow open depth were interlocked and had some connectivity, whereas in the simulation, they were set to be perfectly disconnected. It was challenging to simulate the electrical properties of the interfaces between the cement composite and mortar and between the mortar and rebar. Moreover, the resistance of the mortar changes over time due to polarization and ion flow, but this was ignored in this simulation. Therefore, when comparing the experiment and simulation results, it is more appropriate to find the tendency of change in resistance due to various conditions, such as the effects of cracks and their moisture content, rather than comparing absolute resistance values.

4. Results

4.1. Effect of moistures

Fig. 13 shows the change in resistance of CNT-CF/cement composite sensors embedded in the mortar specimen (S meas) for Test M and those between the adjacent composite sensors (H meas) during drying. The changes in relative humidity and temperature inside and outside of the specimens are also presented. Along with the decrease in external humidity from 100% to 20% by air drying and accelerated drying by silica gel, the internal relative humidity of the mortar surrounding the composite sensors gradually reduced from 100% to 50%. Although there might be a slight difference between the internal relative humidity value measured by the probe-type sensor and the embedded composite sensor or its surrounding mortar, it was expected that significant drying occurred for the composite sensors and surrounding mortar.

The experimental results show that the resistance of the composite sensors was not affected by the relative humidity. While the internal relative humidity of mortar was reduced from 100% to 50%, the S meas resistance results only varied by up to 10% at the $2 \times 10\ \Omega$. Considering that the change in resistance value generally occurs on a logarithmic scale, this difference is considered negligible. This can be attributed to the electrical resistivity of the composites in the present work which was extremely lower than those from other works [16]. In the case of our previous work [17], the mixture with poor CNT dispersibility showed a difference in resistance value by 10 times depending on the moisture.

The resistance of H meas also showed little change depending on the drying conditions, similar to the value of S meas. The resistance of H meas indicates the resistance of the surrounding mortar, and the cement composites act as electrodes for them. The approximate initial resistance value was within a range of 10^3–$10^4\ \Omega$, and in some cases, intermittent increases or decreases in the results from about 10 times to 1/10 times

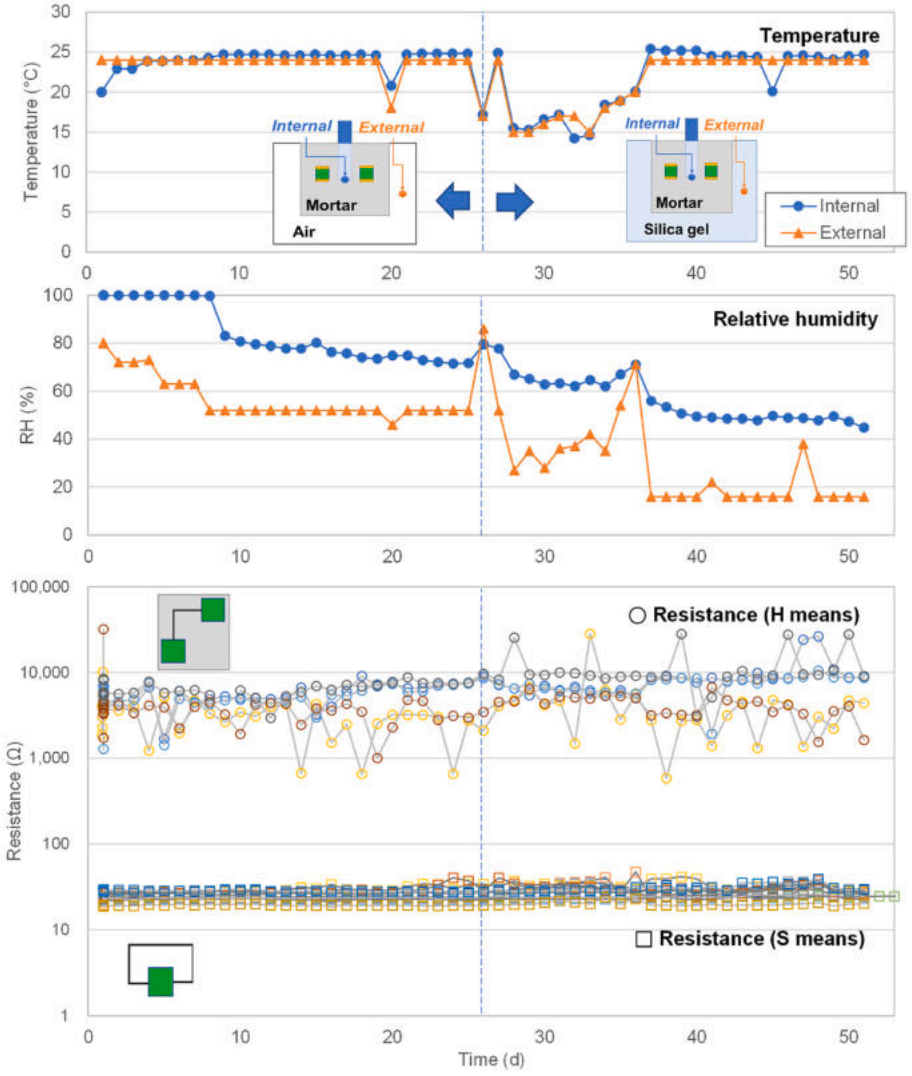

Fig. 13. External temperature, relative humidity, and resistances of the cement composites (S meas) and the mortar surrounding them (H meas) for Test M.

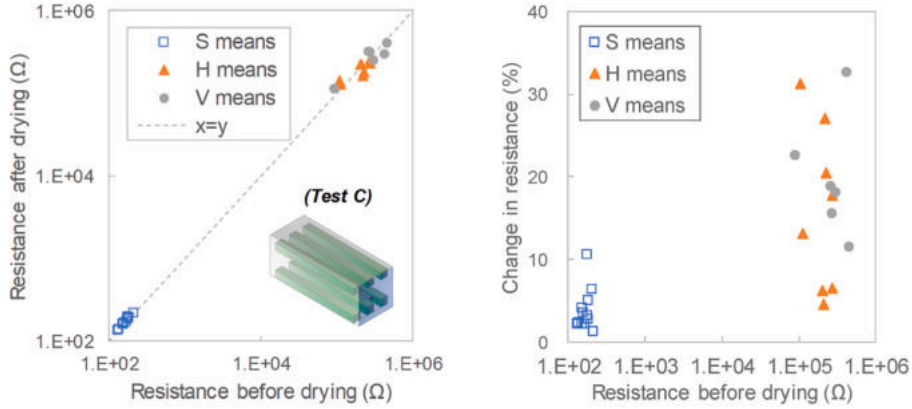

Fig. 14. Measured resistances of the cement composites (S meas) and the mortar surrounding them (H and V meas) for Test C after drying (left) and their change in resistance by drying (right).

were found. This fluctuation range is a common error when measuring the electrical conductivity of mortar or concrete by the 2-probe method [18]. However, as listed in Table 1, the resistivity of the mortar at saturated condition and that at vacuum-dried with 50 °C for 3 days showed a larger difference. This is presumably because the drying method used in Test M was not as harsh as high-temperature vacuum drying.

In addition, Fig. 14 shows the resistance values of S, H, and V meas of

Table 3
The electrical properties for the simulation.

Parameter	Value	Remarks
Resistivity of mortar	Max 5.5×10^5 Ω·m (dried specimen) Min 5.5×10^2 Ω·m (saturated specimen)	Table 1 in the present work
Resistivity of CNT-CF cement composite	0.09 Ω·m	
Resistivity of rebar (reinforcement steel bar)	2.48×10^{-7} Ω·m	Software database
Relative permittivity of mortar	2	Modified from [14]
Relative permittivity of CNT-CF cement composite	13	Modified from [15]
Crack width	0.1–1.0 mm	Setup
Resistivity of air (dried crack)	1.0×10^{12} Ω·m	Lowest value for simulation
Resistivity of sea water	2.0×10^{-1} Ω·m	Measured in [7]
Resistivity of tap water	1.0×10^{1} Ω·m	
Resistivity of self-healed crack	Max 1.0×10^{12} Ω·m	Assumed, the value may within a range between those of water and air

Table 4
Summary of relative resistances of parallelly-arranged conductive cement composite sensors in reinforced mortar and those between nearby sensors.

Crack situation	Measured relative resistance per initial values	
	Bar-type single composites sensor (S meas)	Resistance between nearby sensors (H and V meas)
Without crack	0.9–1.1 (Fig. 13)	H/V meas: 0.5–2 (Fig. 13)
New crack, Dry	2-1000 (Fig. 16)[a]	H/V meas: 5-10 (Fig. 17)
New crack, Saturated	0.9–1.1 (Fig. 16)	H/V meas: 0.5–2 (Fig. 17)
After crack, self-healed (filled by efflorescence)	2-10 (Fig. 17)	H/V meas: 2-5 (Fig. 17)
Without crack, after long-term carbonation/chloride penetration [1,13]	10–1000	H/V meas: 2-4
With crack, after long-term carbonation/chloride penetration	No data (to be measured in future work)	No data (to be measured in future work)

[a] Varied by the crack width ranging from 0.01 to 1.0 mm.

the specimen for Test C before cracking, which were measured before and after drying in air. This measurement sequence is explained in Table 3 (Sequences 1 and 2). Drying was carried out in a chamber with a relative humidity of 20% for seven days. As mentioned in Table 3, the time required for drying after cracking was planned for seven days. Therefore, in this case, only seven days of drying were carried out to confirm the effect of moisture. Similar to the results from Test M, the change in electrical resistance of S, H, and V meas after a seven-day drying period was insignificant. For the specimen in Test C, the change in S meas was within 10% compared to the initial values, and within 40% for H and V meas. This result confirms that the change in electrical resistance due to moisture content of the mortar in Test C would be negligible.

4.2. Resistance changes before and after cracking

Fig. 15 shows the change in electrical resistance of S meas for Test C during flexural loading and cracking. As confirmed in literature [19,20], the resistance of the cement composite sensor increased rapidly as cracks occurred. The increased ranges of the resistance values appeared to be relatively proportional to the width of the crack, which was detected by a microscope (Fig. 7). Fig. 16 summarizes the relationships between crack width and the relative resistance of S meas, i.e., the ratio between S meas value after cracking and initial value before cracking. In both the experiment and simulation results, the resistance of S meas increased by a factor of 100 after cracking when the crack was dry. For the experiment result, the value of S meas was gradually increased by the increase in the crack width due to partial connection in actual specimens after cracking, whereas for the simulation result, that was not affected by the crack width. However, when the crack was wet, both experiment and simulation results showed that there was no change in the S meas values due to the electrical connection by water filled in the crack. In addition, the piezoresistive effect, which refers to the resistance changes in response to the tensile strain of the composite sensor before cracking, was difficult to observe in Fig. 15. Prior to cracking, the resistance value remained unchanged despite the composite being under loading, and a rapid increase in resistance was only observed after cracking occurred.

Fig. 17 summarizes the results of the experiment and simulation for S, H, V, and X meas in different cracking situations. The values presented in Fig. 17 are the averages and standard deviations of the results obtained from multiple composite sensors shown in Fig. 5b. The general trends of the experimentally measured S, H, and V meas values agreed with the simulation results. However, differences in resistances of S, H, and V meas between the experiment and simulation were observed, which could be attributed to various factors such as size, interface, and cracking patterns. The resistance of H and V meas increased by 1–8 times and 2-8 times, respectively, compared to the initial value before cracking when the crack was generated and dried. In the case of X meas, the resistance was too high before cracks occurred, and it was displayed as overload since the distance between the working electrodes was significantly larger than that of H and V meas. The difference in tendency between the experiment and simulation results for X meas was significant.

In the wet state after cracking, the resistance values of S, H, and V meas did not significantly differ from those before cracking, indicating that accurate monitoring was impossible with S, H, and V meas if the crack was continuously saturated. However, a significant change in resistance value before and after cracking was observed for X meas. In the case of self-healed cracks, the resistances of all S, H, and V meas increased compared to those before the crack occurred regardless of the dried or wet state. The increase ranges of S, H, and V meas were 2–5 times for the dried state and 1-2 times for the wet state. Note that the simulation results of S, H, and V meas after the crack was self-healed could vary widely depending on the input values of resistance for the crack.

Fig. 18 presents simulated resistances of S, H, V, and X meas for various crack widths and filling conditions. When the crack width was changed through simulation, the change in each electrical resistance value according to the crack width was negligible, as also shown in Fig. 16. The application of sea water in the crack resulted in a decrease in resistance due to the higher electrical conductivity of the sea water compared to cement composites. Fig. 19 presents the simulation results of resistance of S, H, V, and X meas of the specimen with and without rebar. The effect of rebars on the resistances from the composites was also not significant. The effect of reinforcing bars on the H and V meas

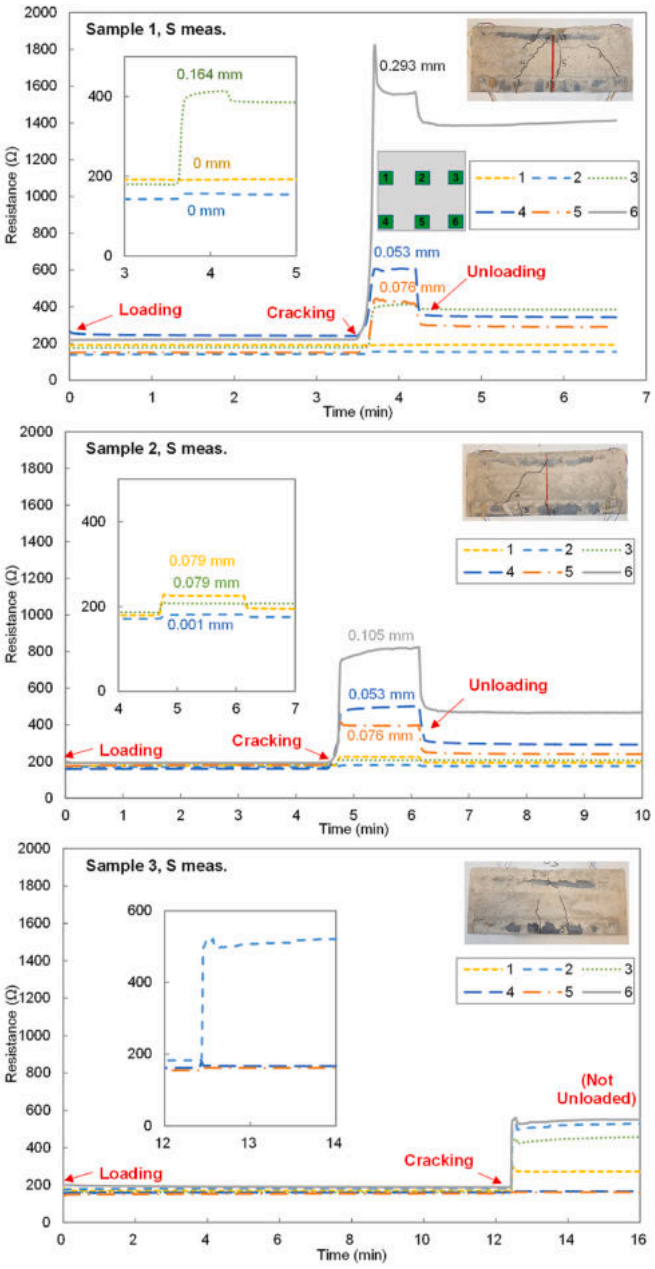

Fig. 15. Measured resistivity change (S means) of the cement composites embedding in reinforced mortar during three-point bending (numbers in graph: maximum crack width on the composites at surface).

values was negligible, while the difference in resistance was significant for S meas only when the crack was dry. As illustrated in Fig. 20, which is redrawn from the simulation results in Figs. 11 and 12, the rebar seldom affected the current flow between parallelly-arranged composite sensors.

5. Discussion: monitoring strategy

Table 4 summarizes the results of experiments and simulations conducted in this work. Additionally, Table 4 includes the effects of chloride permeation and carbonation on the resistances of parallelly-arranged CNT-CF/cement composite sensors, which were experimentally confirmed in Refs. [1,13]. Based on the results in Table 4, Table 5 proposes strategies for predicting the state of concrete based on sensor signals.

For sound concrete structures with no cracks and no carbonation or chloride penetration, the S meas value (resistance of the composite sensors) remains relatively constant. While the H and V meas values, i.e., the resistance of the surrounding concrete, may slightly fluctuate depending on mortar humidity, their fluctuation ranges are within 1/2 to 2 times. However, if the crack is exposed to wet-dry cycles during service life, all S, V, and H meas values will fluctuate greatly (2-10 times). In a constantly saturated condition, S, V, and H meas values do not change from the state before cracking. In this case, monitoring X meas values is necessary, although the reliability of this signal is not high. However, after sufficient time has passed for some hydration products to form between the crack, which is self-healing, the S, V, and H meas values increase compared to their initial values by up to 2-10 times and more. This means that monitoring the crack is possible with this strategy. Furthermore, as shown in Table 4, carbonation and

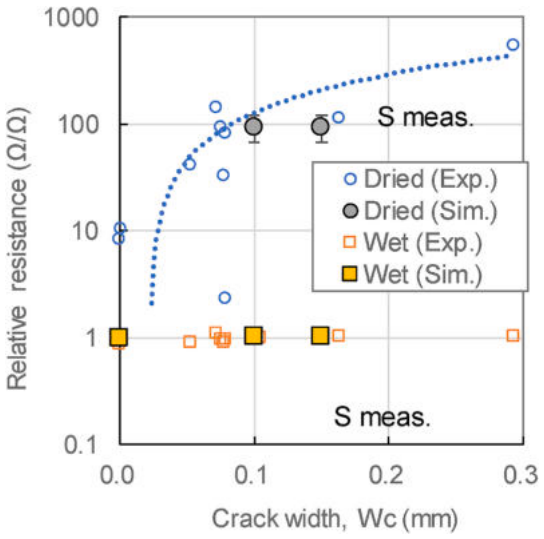

Fig. 16. Crack width vs. change in resistances of the cement composite (S meas.) embedded in reinforced mortar during after three-point bending: experimental and simulation results.

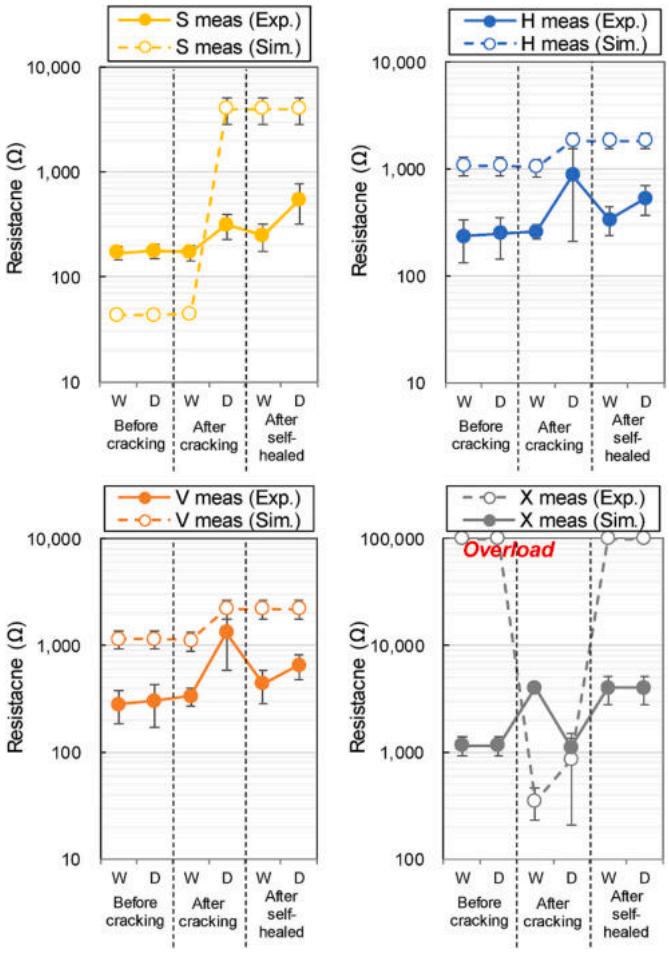

Fig. 17. Measured and simulated resistances of the cement composites and the surrounding mortar in various situations (Crack width: 0.02–0.15 mm, W or D: wet or dried in the crack).

chloride ion penetration can significantly increase the values of S, V, and H meas. This means that by detecting the increase or fluctuation of the values of S, V, and H meas, it is possible to monitor the cracking of the concrete structures as well as carbonation and chloride attacks. If the resistance of the high-conductive cement composite installed at the same depth as rebars changes, it could indicate that cracks have

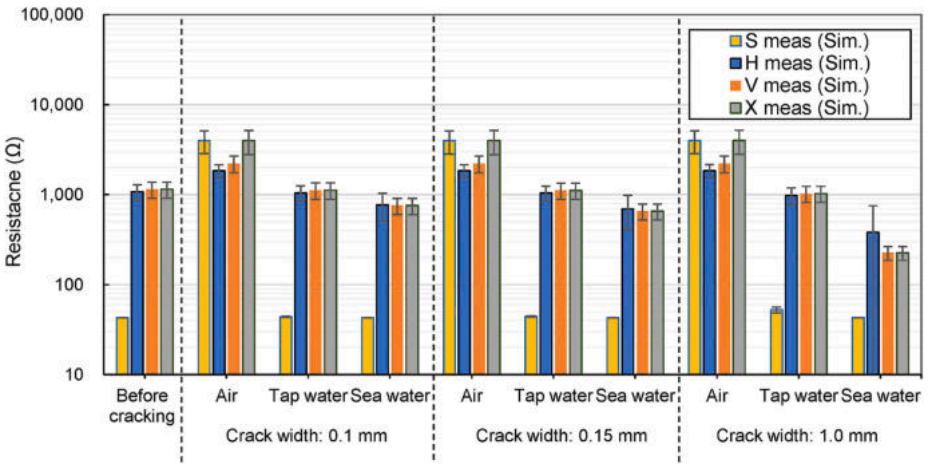

Fig. 18. Simulated resistances of the cement composites and the surrounding mortar having crack widths of 0.1 mm, 0.15 mm, and 1.0 mm, filled with air (dried), tap water, and sea water.

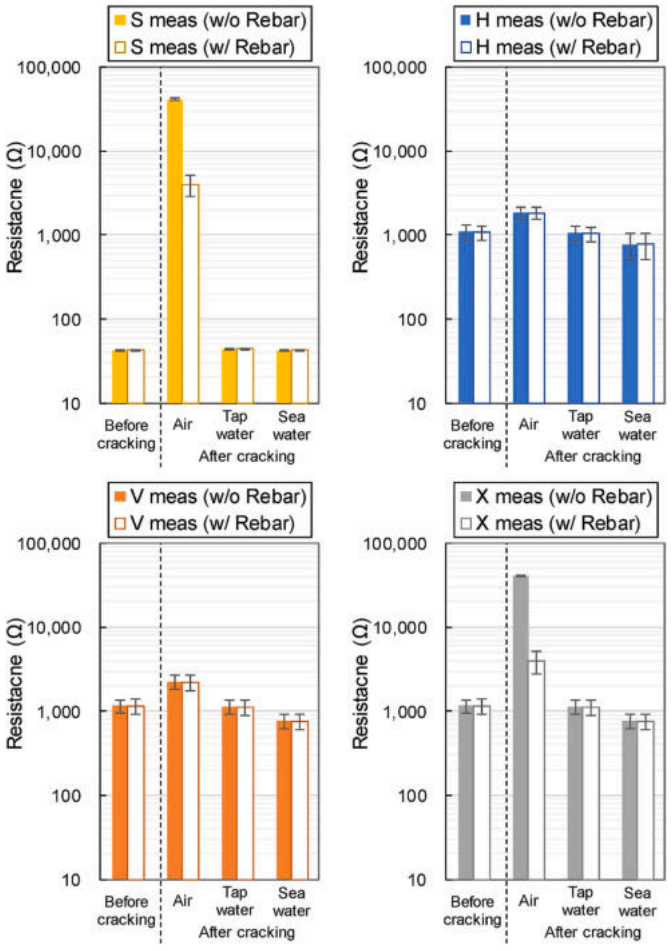

Fig. 19. Simulated resistances of the cement composites and the surrounding mortar in various situations (Crack width: 0.1 mm): specimen with and without rebar.

occurred around the rebars or that the carbonation depth or chloride ion penetration depth has reached that position.

In summary, the mechanism for monitoring cracks via multiple conductive cement composite sensors is essentially the same as with a single sensor, as the resistance of composite sensors increases and/or fluctuates when cracking occurs. However, when using a single sensor,

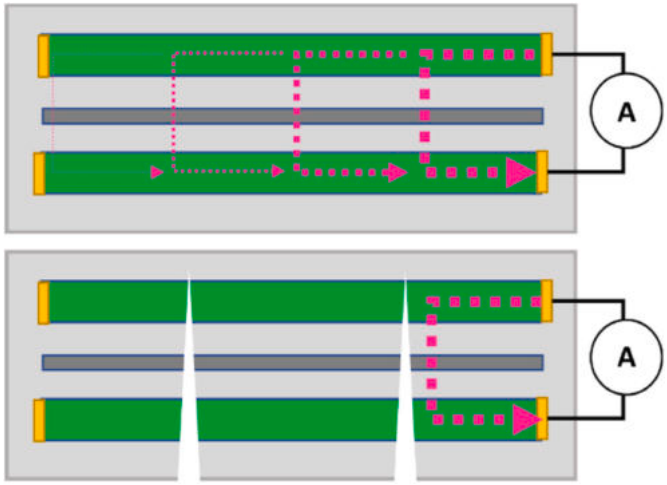

Fig. 20. Schematic of current flow direction and current density between parallelly-arranged conductive cement composite sensors before and after cracking.

only one result can be obtained, whereas using two or more sensors can provide more signals, including those for each composite sensor and those between adjacent composite sensors. Therefore, using multiple composite sensors is a more reliable method for monitoring cracks in concrete structures.

One limitation of this study is that the threshold value for accurate judgment was not presented. It was confirmed in a short-term laboratory experiment that when damage occurs to a concrete structure, the S, V, and H meas from the cement composite sensors fluctuated by more than twice the initial value. However, since cracks are more likely to occur over a long period of time in real structures, it is necessary to establish a clearer threshold level through scale-up experiments in order to obtain accurate results. Moreover, the design and installation issues of the proposed sensors for the practical concrete structures should be considered. If the cracks on the concrete structure do not intersect the sensor, it is impossible to monitor the cracking via the proposed method. Considering the application, the shape, length, and interval of multiple cement composite sensors should be determined. These issues will be studied in the future work.

Table 5
Strategy of crack monitoring for concrete structure via parallelly-arranged conductive cement composite sensors.

Time-dependent trend of resistance (relative resistance per initial value)		Expected crack condition	Rebar corrosion potential
Bar-type single composites sensor, S meas	Resistance between nearby sensors, H and V meas (=resistance of surrounding concrete)		
Initial range, constant (0.9–1.1)	Initial range, constant (0.5–2)	No cracks, or cracks saturated after formation	No
Increased, fluctuating[a] (0.9–100)	Increased, fluctuating (0.9–10)	Crack generated, under wet-dry cycle	High
Increased, constant[a] (2-100)	Increased, constant[a] (2-10)	Crack generated, continuously dry	Low, but continuous inspection required
Increased, fluctuating[a] (2-10)	Increased, fluctuating[a] (2-10)	Crack generated, usually wet, but self-healed	Low, but continuous inspection required
Increased, constant[b] (10-1000)	Increased, constant (2-5)	Chloride penetration, carbonation, no cracks	lower than the case of open crack (Inspection required)

[a] Resistance fluctuation induced by moisture content (the crack width 0.01–1.0 mm).
[b] Increase range of resistance of the single composites was much higher than surrounding mortar or concrete.

6. Conclusion

In this study, a crack monitoring strategy using parallelly-arranged multiple conductive cement composites for reinforced concrete was verified through a series of experiments and simulations. The following conclusions have been drawn:

1) The experimental results show that the resistance of the composite sensors was not affected by the relative humidity. While the internal relative humidity of mortar was reduced from 100% to 50%, the resistance of the composite sensor only varied by up to 10% at the 2×10 Ω. The resistance of surrounding mortar detected by two composite sensors also showed little change depending on the drying conditions. In the experimental setting of this work, the approximate initial resistance values between the composite sensors embedded in the reinforced mortar with a 30 mm gap were within a range of 10^3–10^4 Ω, although intermittent increases or decreases in the results from about 10 times to 1/10 times were found.
2) The resistance of the cement composite sensor increased rapidly as cracks occurred. The increased ranges of the resistance values appeared to be relatively proportional to the width of the crack. The averaged resistances of surrounding mortar detected by two composite sensors also increased by 2–10 times, respectively, compared to the initial value before cracking, when the crack was generated and dried. However, in the wet state directly after cracking, the resistance values of the composite sensors and those between two sensors did not significantly differ from those before cracking when the crack was continuously saturated. In the case of self-healed cracks, the resistances of the composite sensors and those between two sensors increased compared to those before the crack occurred regardless of the dried or wet state. The general trends of the experimentally measured values agreed with the simulation results.
3) The strategy for monitoring cracks via multiple conductive cement composite sensors is essentially the same as with a single sensor, as the resistance of composite sensors increases and fluctuates when cracking occurs. However, when using a single sensor, only one result can be obtained, whereas using two or more sensors can provide more signals, including those for each composite sensor and those between adjacent composite sensors, i.e., resistance of the mortar. Therefore, using multiple composite sensors is a more reliable method for monitoring cracks in concrete structures.

Declaration of competing interest

The authors declare that they have no known competing financial interests or personal relationships that could have appeared to influence the work reported in this paper.

Data availability

Data will be made available on request.

Acknowledgement

This research was supported by grants from the Ministry of Trade, Industry & Energy [RS-2022-00155662], “Regional Innovation Strategy (RIS)" through the National Research Foundation of Korea (NRF) funded by the Ministry of Education (MOE) [2021RIS-002], the National Research Foundation of Korea (NRF-2021R1A4A3033128) funded by the Ministry of Science and ICT, and Chosun University (2023). Authors also appreciate to undergraduate students in Chosun University for their help on fabrication of specimens. The opinions expressed in this paper are those of the authors and do not necessarily reflect the views of the sponsor.

Appendix

Table A1
Mesh statistics for cracked specimens

Description	Value
Status	Complete mesh
Mesh vertices	347,552
Tetrahedra	2,045,093
Triangles	351,724
Edge elements	4,693
Vertex elements	122
Number of elements	2,045,093

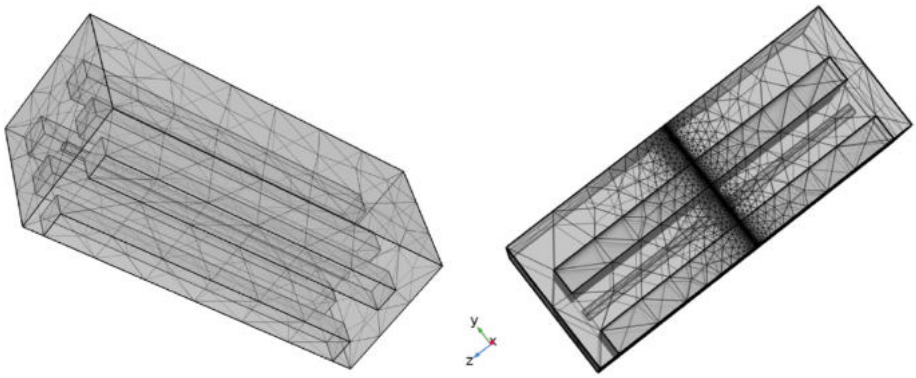

Fig. A1. Mesh for cracked specimens

References

[1] H.K. Lee, et al., Fluctuation of electrical properties of carbon-based nanomaterials/cement composites: case studies and parametric modeling, Cement Concr. Compos. 102 (2019) 55–70.

[2] A. Yazdanbakhsh, Z. Grasley, The theoretical maximum achievable dispersion of nanoinclusions in cement paste, Cement Concr. Res. 42 (6) (2012) 798–804.

[3] S. Wansom, et al., AC-impedance response of multi-walled carbon nanotube/cement composites, Cement Concr. Compos. 28 (6) (2006) 509–519.

[4] N.K. Lee, et al., Electrical resistivity stability of CNT/cement composites after further hydration: a simple evaluation with an accelerated method, Construct. Build. Mater. 317 (2022), 125830.

[5] W. Dong, et al., Multifunctional cementitious composites with integrated self-sensing and hydrophobic capacities toward smart structural health monitoring, Cement Concr. Compos. 118 (2021), 103962.

[6] W. Dong, et al., Piezoresistive performance of hydrophobic cement-based sensors under moisture and chloride-rich environments, Cement Concr. Compos. 126 (2022), 104379.

[7] M.-J. Lim, et al., Carbon nanotube/cement composites for crack monitoring of concrete structures, Compos. Struct. 180 (2017) 741–750.

[8] Y. Ding, et al., Concrete with triphasic conductive materials for self-monitoring of cracking development subjected to flexure, Compos. Struct. 138 (2016) 184–191.

[9] M. Chen, et al., Mechanical and smart properties of carbon fiber and graphite conductive concrete for internal damage monitoring of structure, Construct. Build. Mater. 142 (2017) 320–327.

[10] A. Downey, et al., Damage detection, localization and quantification in conductive smart concrete structures using a resistor mesh model, Eng. Struct. 148 (2017) 924–935.

[11] A. Downey, et al., Automated crack detection in conductive smart-concrete structures using a resistor mesh model, Meas. Sci. Technol. 29 (3) (2018), 035107.

[12] M. Pour-Ghaz, J. Weiss, Detecting the time and location of cracks using electrically conductive surfaces, Cement Concr. Compos. 33 (1) (2011) 116–123.

[13] M. Tafesse, et al., Effect of chloride penetration on electrical resistivity of CNT–CF/cement composites and its application as chloride sensor for reinforced mortar, Cement Concr. Compos. 133 (2022), 104662.

[14] P. Juan-García, J. Torrents, Measurement of mortar permittivity during setting using a coplanar waveguide, Meas. Sci. Technol. 21 (4) (2010), 045702.

[15] J.-K. Yuan, et al., Giant dielectric permittivity nanocomposites: realizing true potential of pristine carbon nanotubes in polyvinylidene fluoride matrix through an enhanced interfacial interaction, J. Phys. Chem. C 115 (13) (2011) 5515–5521.

[16] G. Hong, et al., Moisture dependence of electrical resistivity in under-percolated cement-based composites with multi-walled carbon nanotubes, J. Mater. Res. Technol. 16 (2022) 47–58.

[17] H. Kim, I. Park, H.-K. Lee, Improved piezoresistive sensitivity and stability of CNT/cement mortar composites with low water–binder ratio, Compos. Struct. 116 (2014) 713–719.

[18] M. Tafesse, et al., Flowability and electrical properties of cement composites with mechanical dispersion of carbon nanotube, Construct. Build. Mater. 293 (2021), 123436.

[19] R. Ranade, et al., Influence of micro-cracking on the composite resistivity of engineered cementitious composites, Cement Concr. Res. 58 (2014) 1–12.

[20] C. Boulay, S. Dal Pont, P. Belin, Real-time evolution of electrical resistance in cracking concrete, Cement Concr. Res. 39 (9) (2009) 825–831.